Research Article Vol. 34, No. 4 / 23 Feb 2026 / Optics Express 5833
Optics EXPRESS

Intensity noise suppression in pulsed lasers via combining relaxation oscillation with nonlinear frequency conversion

JIE YANG,[1,†] YANLIN ZHANG,[2,†] WEIJIE LI,[1] XIAOJUN JIA,[1,3] HUADONG LU,[1,3,*] AND KUNCHI PENG[1,3]

[1]State Key Laboratory of Quantum Optics Technologies and Devices, Institute of Opto-Electronics, Shanxi University, Taiyuan 030006, China
[2]Institute of Molecular Science, Shanxi University, Taiyuan 030006, China
[3]Collaborative Innovation Center of Extreme Optics, Shanxi University, Taiyuan 030006, China
[†]These authors contributed equally to this work
[*]luhuadong@sxu.edu.cn

Abstract: This paper reports a method for reducing the relative intensity noise (RIN) of actively Q-switched pulsed laser by combining the relaxation oscillation (RO) and nonlinear optical frequency conversion (NOFC). When a RO is introduced by slightly lowering the diffraction loss of acousto-optic (AO) Q-switch, the initial population inversion per pulse is stabilized to a constant value by the RO process. The RIN between pulses decreases from 4.90% to 2.48% by optimizing the diffraction loss of AO Q-switch and the RO duration. On this basis, the NOFC is introduced into the cavity by a noncritical phase-matched nonlinear crystal LiB_3O_5 (LBO) to further suppress the intensity fluctuation arising from different longitudinal-mode beating with random phases, and the RIN further decreases to 1.30%, corresponding to a pulse energy stability of 0.09%. This is the lowest RIN between pulses in large energy Q-switched lasers, to the best of our knowledge. The proposed method paves the way to effectively suppress the RIN of pulsed lasers, which will help us to explore what we believe to be many new physical phenomena due to their high peak power and available manipulation in time dimension.

© 2026 Optica Publishing Group under the terms of the Optica Open Access Publishing Agreement

1. Introduction

It is well known that a single-longitudinal-mode (SLM) all-solid-state continuous-wave (CW) laser is always an irreplaceable source in cold atom physics, laser spectroscopy, quantum teleportation and gravitational wave detection [1,2] owing to its exceptionally low intensity noise. However, when the output power of a SLM CW laser is scaled up by increasing the incident pump power, the severe thermal effect and the intense mode-competition can restrict its output performance including limiting the output power [3], increasing the intensity noise, degenerating the beam quality and so on. In order to address this issue, a nonlinear loss was introduced to a unidirectional ring resonator including several laser crystals and the output power was scaled up to 140 W [4]. Moreover, the introduced nonlinear loss effectively suppressed the intensity noise of the laser at the frequency of resonant relaxation oscillation (RRO) [5–9]. Nevertheless, further power improvement of the SLM CW laser depends only on the laser amplifier, such as the main oscillation power amplifier (MOPA) and seed-injection locking, which can increase the complexity of the system [10–12]. In contrast to the CW lasers, pulsed lasers present the promising alternatives with higher peak power (kilowatts to megawatts) and less thermal load. Additionally, their unique temporal controllability extends their ability to frontier research such as lidar, nonlinear optics, and plasma physics [13]. However, compared to CW lasers, pulsed lasers exhibit more complex noise characteristics due to the intrinsically stochastic nature of pulse building-up [14–16]. Consequently, on the basis of improving the output power stability, it is paid more attention to stringently controlling fluctuations in pulse

#586251 https://doi.org/10.1364/OE.586251
Journal © 2026 Received 28 Nov 2025; revised 27 Jan 2026; accepted 2 Feb 2026; published 9 Feb 2026

Optics EXPRESS

energy, pulse intensity and pulse timing. As early as 1990, Jeffrey A. et al. inserted an etalon into the resonator of a pulsed laser which employed a saturable absorber as the passive Q-switch to achieve SLM operation and simultaneously reduce the intensity fluctuations from 10% to approximately 2%. However, the single-pulse energy and peak power were limited to 20 μJ and 1 kW, respectively [17]. In 2012, Shigeki Matsuo et al. employed a Kerr medium to establish an optical negative-feedback mechanism and further reduce the energy fluctuation of a mode-locked laser from 1.13% to 0.47% [18]. However, the presented method strongly depended on the third-order nonlinear susceptibility, thickness, and irradiance of the Kerr medium, which directly restricted its applicability to a specific pulse energy regime of about 1.7 μJ. Unlike passively Q-switched lasers or mode-locked lasers, in actively Q-switched lasers, the pulse building-up can be effectively controlled by employing a precise external radio frequency (RF) driver, so it is easy to achieve both higher peak power and lower intensity noise. In 2005, Hengli Zhang et al. reported an actively electro-optic Q-switched pulsed laser by inserting a BBO electro-optic crystal into an off-axis negative-branch confocal unstable hybrid resonator. At the same time, a cylindrical lens was employed to compensate for the thermal lensing effect of the gain medium and then achieve the goal of thermal unsensitivity. The output energy, pulse width and corresponding peak power were 25 mJ, 22.4 ns and 1.11 MW, respectively. However, the pulse energy fluctuation was as high as 0.8% [19]. In 2025, our group presented a SLM actively Q-switched 1064 nm laser by introducing a nonlinear loss into the resonator to suppress the sub-modes oscillation [20]. However, we didn't pay more attention to the RIN of the laser.

In order to effectively suppress the relative intensity noise (RIN) of an actively Q-switched laser with high peak power, in this paper, we presented what we believe to be a novel method which was achieved by combining a relaxation oscillation (RO) with the nonlinear optical frequency conversion (NOFC). The diffraction loss of the acousto-optic (AO) Q-switch was firstly lowered to allow lasing at the end of the pump period. At this time, all pulses experienced a RO process before their building-up. In this case, the inverted population and photons evolve toward the steady states, the inverted population at the beginning of pulse building-up was stabilized to the threshold population inversion where the gain was equal to the total loss of the resonator. In other words, the net gain of the subsequent pulses was exactly the same as that of the first pulse, which meant that the first pulse was completely replicated by the subsequent pulses. As a result, the intensity fluctuations between the pulses could be effectively suppressed. On this basis, NOFC was then introduced to further suppress the intensity fluctuation caused by the different longitudinal-mode beating with random phases. At last, the pulse-to-pulse RIN was reduced from 4.90% to 1.30%, and the achieved responding pulse energy stability was better than 0.09%.

2. Fundamental principles

Figure 1(a) shows the dynamics of a conventional actively Q-switched laser, where n, η, and ϕ represent the inversion population, the diffraction loss of the AO Q-switch and intracavity photons, respectively. When the incident pump laser is injected into the resonator and the maximum value of η is adopted, a large number of active ions in the gain medium are excited to the upper energy level and thereby the population inversion is formed in the period of T_1. At the moment, when η is removed, a pulse quickly builds up with the high peak power and leaks from the output coupler of the resonator in the period of T_2. However, due to the fluctuations of inverted population caused by the pump power fluctuation, time jitter of the Q-switch and so on, the peak powers between pulses are so different that the significant intensity noise in the pulsed laser is easily observed. To overcome this problem, the diffraction loss η of the AO Q-switch is designedly set to be slightly lower than that in Fig. 1(a), which is depicted in Fig. 1(b). A RO process with the period of T_{12} can be introduced after the sufficient inverted population is accumulated in the period of T_{11}, which means that the period of T_1 shown in Fig. 1(a) will be divided into two periods including T_{11} and T_{12}. Especially, in the period of T_{12}, with the introduction of the

Optics EXPRESS

RO, both the inverted population n and photons ϕ will evolve toward a steady state where the gain equals the total loss including cavity loss and η, whose principle is similar to that of the continuous-wave lasers. At the end of T_{12}, once η is removed, a stable pulse train with low RIN is achieved.

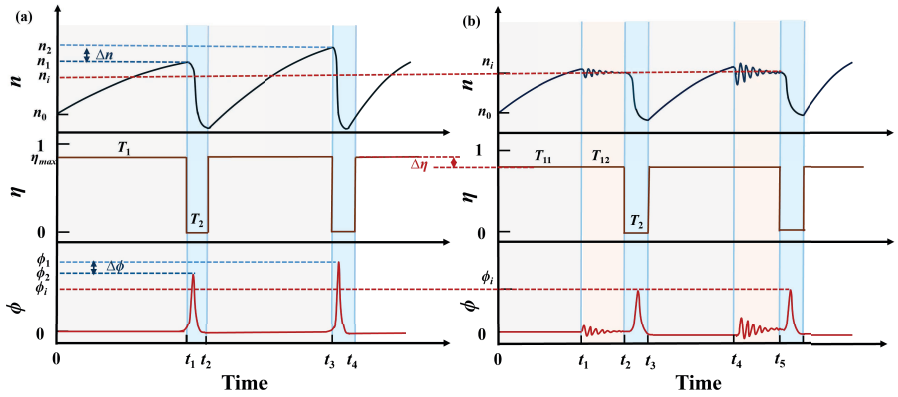

Fig. 1. The laser dynamics of conventional actively Q-switched lasers (a) and population inversion stabilization mechanism by RO (b)

In order to analyze the influence of RO on inverted populations in detail, the dynamics presented above are simulated using the rate equations. For a ring laser resonator, the rate equations are given by:

$$\begin{cases} \dfrac{\mathrm{d}n}{\mathrm{d}t} = -\gamma c\phi n - \dfrac{n}{\tau_c} + P, \\ \dfrac{\mathrm{d}\phi}{\mathrm{d}t} = \dfrac{\phi}{t_r}\left\{\sigma n l - \left[\ln\left(\dfrac{1}{R}\right) + \delta\right]\right\} + S. \end{cases} \tag{1}$$

here, ϕ denotes the intracavity photon number density, and n represents the inverted population density within the gain medium. R denotes the reflectivity of the output coupler, while δ represents the round-trip loss factor, incorporating losses due to diffraction, scattering, and absorption. t_r is the cavity round-trip time, c is the speed of light in vacuum, and τ_c is the fluorescence lifetime of the gain medium. P represents the pumping rate. The parameter S is the fraction of spontaneous emission photons that enter the lasing mode, representing the spontaneous emission contribution to stimulated emission.

Figure 2 shows the simulated dynamics with and without RO from numerically solving Eq. (1) using the Runge-Kutta method. The gain medium was selected as Nd:YVO_4 pumped by a laser diode (LD) at the wavelength of 888 nm. The output power and the duration of LD are set to 120 W and 300 μs, respectively. In order to study the effect of inverted population fluctuation on the pulse intensity, a 10% fluctuation (−5%, 0% and +5%) from the fluctuations of pump power, thermal lens and Q-switch jitter is added to the inverted population between pulses at the end of T_{11} (corresponding to Fig. 1). The diffraction loss of the AO Q-switch is firstly set to the maximum value (85%). In this case, once the loss of diffraction is removed, the large inverted population will decrease quickly since the RO isn't introduced, as shown in Fig. 2(a_1). At the same time, the larger inverted population will cause an earlier pulse building-up and a higher peak power, as shown in Fig. 2(a_2). As a result, the percentage of pulse peak fluctuation is as high as 14.6%, which means that the inverted population fluctuation between pulses will be transferred to peak power by 1.46 times. In contrast, when the diffraction loss of the AO Q-switch is lowered to 82%, the inverted population will not decrease quickly but experience a slow process of RO, as shown in Fig. 2(b_1). In this case, the fluctuation percentage of n is

Optics EXPRESS

stabilized from 10.0% to only 0.007% after the RO process. On this basis, the percentage of pulse peak fluctuation is also reduced from 14.6% to 0.005%, as shown in Fig. 2(b_2).

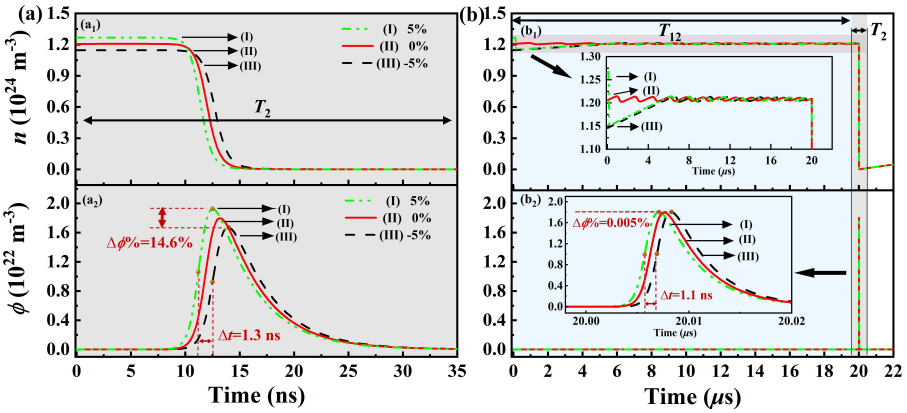

Fig. 2. Simulation dynamic without RO (a) and with RO (b) when the initial inverted population n is given with a fluctuation of −5% (I), 0% (II) and +5% (III), respectively.

The quantified influence of inverted population fluctuation between pulses on the pulse-to-pulse RIN is also simulated, as shown in Fig. 3. For the convenience of comparison, a general calculation method is employed for evaluating the intensity noise under different parameters. This general calculation method is expressed as follows:

$$RIN = \frac{\sigma}{\mu} \tag{2}$$

where σ and μ denote the values of standard deviation and mean, respectively.

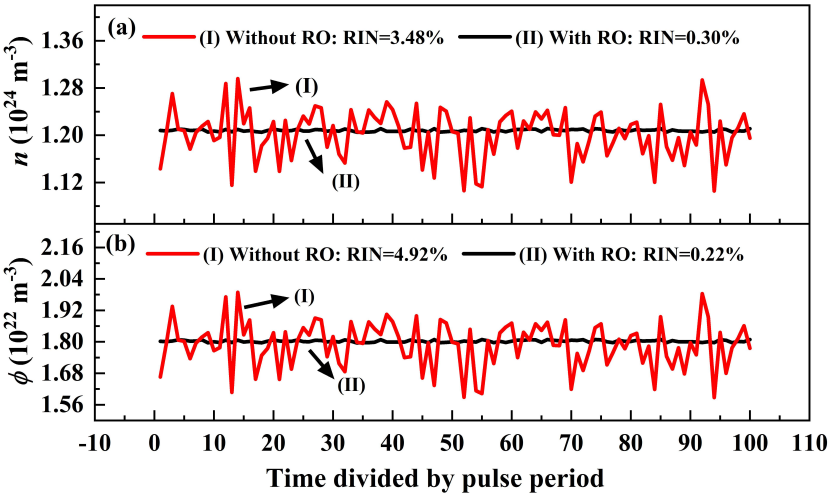

Fig. 3. Simulated pulse-to-pulse RIN without RO (curve (I)) and with RO (curve (II)) when the initial inverted population n is given with a random fluctuation of 10.0%.

Therefore, when the pulse number is set to 100 and the random inverted population fluctuation between pulses is still 10.0%, the RIN of inverted population between pulses is calculated to be 3.48% according to Eq. (2). In this case, after the RO is introduced, the RIN of inverted

Optics EXPRESS

population is reduced from 3.48% to 0.30%, as shown in Fig. 3(a). The RIN of pulse peak is reduced from 4.92% to 0.22%, as shown in Fig. 3(b). The pulse peak fluctuation is 1.4 times that of inverted population fluctuation, which is consistent with Fig. 2.

3. Experimental setup

The proposed method was experimentally verified using a unidirectional ring cavity, as illustrated in Fig. 4. An a-cut, single-end-bonded composite YVO_4/Nd:YVO_4 crystal served as the gain medium, which was directly end-pumped by a laser diode with a center wavelength of 888 nm and a peak power of 200 W, respectively. The polarization-independent absorption at 888 nm in Nd:YVO_4 ensured the uniform gain and thermal distribution within the crystal, enabling high-beam-quality laser output under high pump power. The crystal dimension was $3\times3\times(3+17)$ mm^3, comprising a 17-mm-long doped segment (0.8 at.%) and a 3-mm-long undoped segment. A 1.5° wedge was cut on the rear face of the crystal to introduce a high geometric loss for σ-polarized light and then enhance the polarization purity of the output laser. To reduce the spontaneous emission noise and prevent the thermal damage of the gain crystal, a pulsed pumping scheme operating at a 1 kHz repetition rate with a 300 μs pump duration was employed. The pump light was coupled into the crystal using a telescopic system consisting of two plano-convex lenses with focal lengths of f_1 = 30 mm and f_2 = 100 mm, respectively. The resonator was configured as a four-mirror bow-tie ring cavity. M_1 and M_2 were both plano-convex mirrors with the curvature radii of 1500 mm. The plano-surface was coated with the anti-reflection (AR) film at 888 nm. The convex surface was coated with films of AR at 888 nm and high-reflection (HR) at 1064 nm. M_3 was a flat mirror coated with the HR film at 1064 nm. M_4 served as the output coupler with the transmission of 50% at 1064 nm and high transmission (HT) at 532 nm. To ensure unidirectional operation, an optical unidirectional device composed of a 45° rotator and a $\lambda/2$ waveplate was inserted into the resonant cavity. A stable AO Q-switch (GOOCH & HOUSEGO, QS041-10G-IN2) with 85% maximum diffraction efficiency was employed to accomplish the pulse generation. At the same time, it was used to modulate the cavity loss by controlling the RF power of its driver (CASTECH, CARD-FD2-041-24D24C-1AH-AF). In this case, it was easy to introduce the RO and the laser output performance of the achieved pulsed laser could be manipulated and optimized through real-time electrical signal programming. To suppress intensity fluctuations caused by the multi-longitudinal-mode (MLM) beating, a type-I noncritically phase-matched LiB_3O_5 (LBO) crystal (θ = 90°, ϕ = 0°; dimensions: $3\times3\times18$ mm^3) was inserted between M_3 and M_4 to introduce nonlinear loss. The pulse-to-pulse RIN was

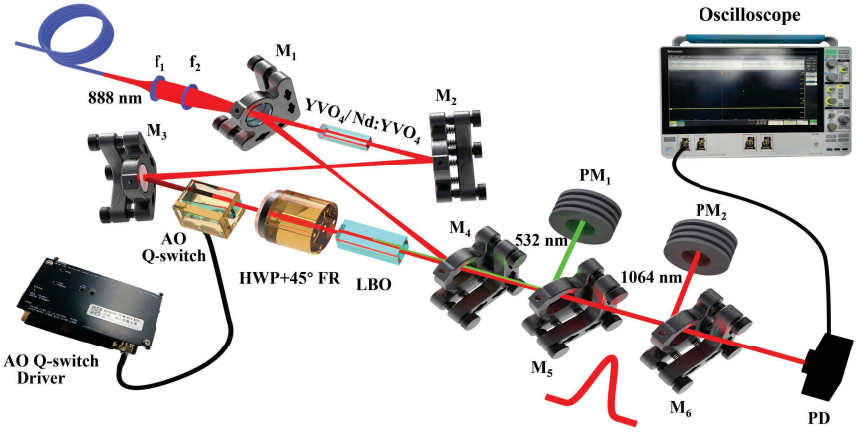

Fig. 4. Experimental schematic for RIN reduction using combined RO and NOFC.

Optics EXPRESS

characterized in the time domain using a fast photodiode detector, and the signal was recorded by a digital oscilloscope (Tektronix, MSO68B) for waveform analysis.

4. Results and discussion

After the whole experimental setup was well-aligned and the diffraction loss of AO Q-switch was set to the maximum of 85%, a pulsed laser with a pulse repetition rate of 1 kHz and a pulse energy of 2 mJ was obtained when the peak power of LD was set to 120 W as well as the repetition rate and duration were optimized to 1 kHz and 300 μs by manipulating the drive current of power supply, respectively, as shown in Fig. 5(a). The pulse-to-pulse RIN was up to 4.90% within 2.25 hours, as shown in Fig. 5(b). It can be seen that the RIN in the conventional actively Q-Switched laser was very high due to the large inverted population fluctuation caused by the pump power fluctuation, time jitter of the Q-switch and so on.

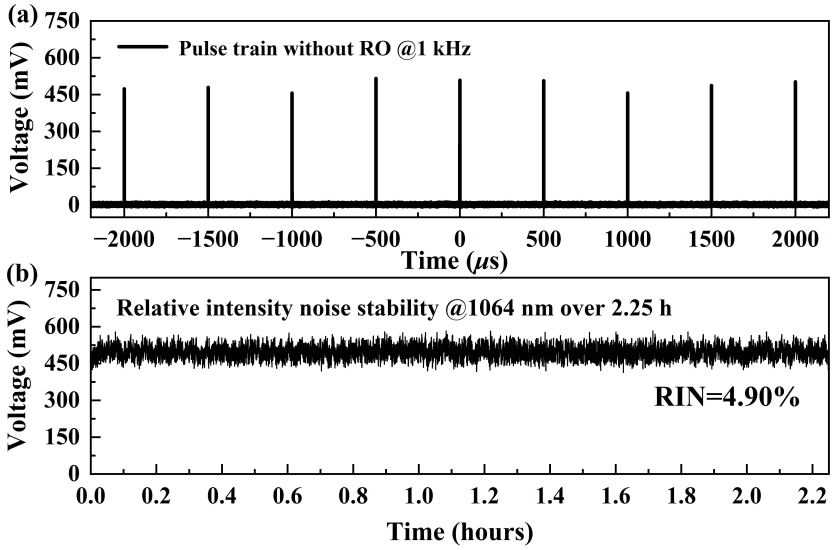

Fig. 5. The pulse-to-pulse RIN without RO. (a) pulse train; (b) RIN within 2.25 hours.

However, when the diffraction loss of AO Q-switch was decreased by decreasing the voltage of the analog signal applied to AO Q-switch from the maximum of 5 V, the RIN of the pulsed laser gradually decreased, which was illustrated in Fig. 6(a). With the decrease of the diffraction loss, the laser threshold gradually reduced and the achieved inverted population began a RO process. When the voltage of the analog signal was decreased to 4.2 V, the diffraction loss of AO Q-switch was only 71% and the minimum RIN of 3.09% was attained, which meant that the inverted population was gradually stabilized to a constant value with the assistance of the RO. When the diffraction loss was further decreased by decreasing the voltage from 4.2 V to 4.0 V, the part of the inverted particles was depleted by the introduced RO process, which significantly reduced the pulse peak value and enlarged the intensity noise. As a result, the RIN of pulse peak value slowly increased from 3.09% to 3.28%. On this basis, the RIN of pulse peak value was further optimized by extending the RO duration experimentally, as shown in Fig. 6(b). It was well known that the RO was a damped oscillation, the longer the RO duration was, the greater stability in the inverted population and photon number at the beginning of pulse building-up was. From Fig. 6(b), when a constant RF drive voltage of 4.2 V was applied to the AO Q-switch, the RIN was reduced from 3.09% to 2.48% when the duration of T_1 (corresponding to Fig. 1) was

Optics EXPRESS

increased from 300 μs to 560 μs. Beyond 560 μs, the RIN plateaued at a stable value because this duration was sufficient for the inverted population to reach a dynamic stable state. When the diffraction loss and the duration of AO Q-switch were optimized to 71% and 560 μs, respectively, it was clear to see that the peak value variation of the pulses was obviously suppressed and the obtained pulse-to-pulse RIN was decreased to 2.48% within 2.25 hours, as shown in Fig. 7.

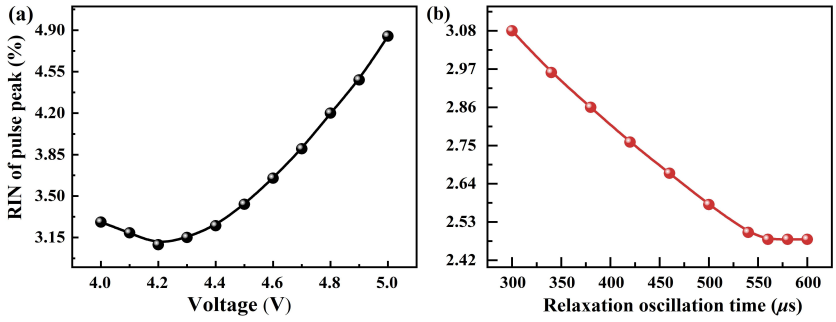

Fig. 6. The variation of RIN with applied signal voltage (a) and the duration of RO (b) under different pump power.

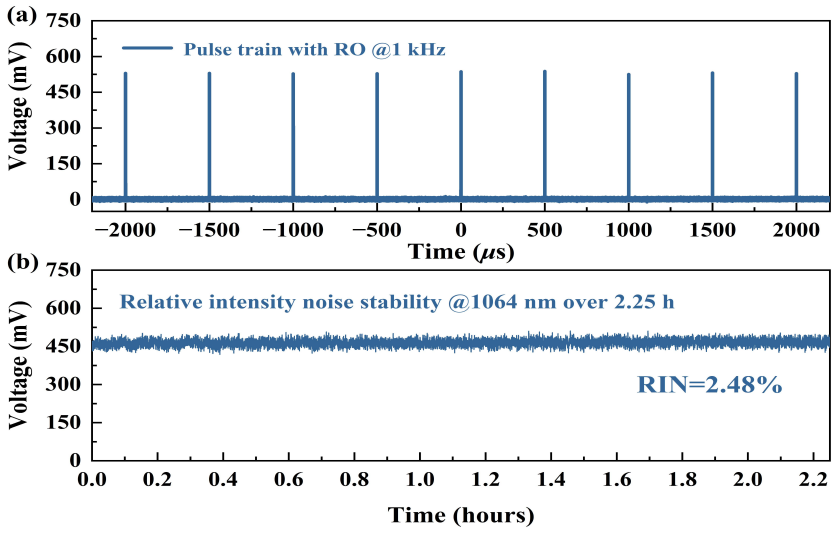

Fig. 7. The pulse-to-pulse RIN with RO. (a) pulse train; (b) RIN within 2.25 hours.

Although the pulse-to-pulse RIN was optimized as much as possible by introducing the RO, the pulse building-up process was often accompanied by beat signal between the different longitudinal-modes (DLMs). In the actively Q-switched lasers, random phases between longitudinal-modes generated heterogeneous pulse shape even if the value of inverted population was the same. To further reduce the RIN by suppressing the mode beating between DLMs, a noncritical phase-matched nonlinear crystal LBO was inserted into the resonator to suppress the oscillation of the sub-modes. The efficiency of NOFC was defined as $\eta = P_{532}/P_{1064}$, representing the ratio of the output power at 532 nm to the fundamental power at 1064 nm outside the cavity. Figure 8 depicted the effect of NOFC on the pulse-to-pulse RIN. As the temperature of the LBO crystal was scanned from 157.50°C to 154.25°C, the maximum efficiency of NOFC occurred at 154.25°C,

Optics EXPRESS

corresponding to the lowest pulse-to-pulse RIN of 1.30%. From the inset, the DLM beating in the pulse waveform was effectively suppressed, resulting in a smooth pulse waveform, which indicated a single longitudinal-mode output. After the sub-modes were effectively suppressed, the RIN decreased from 2.48% to 1.30%.

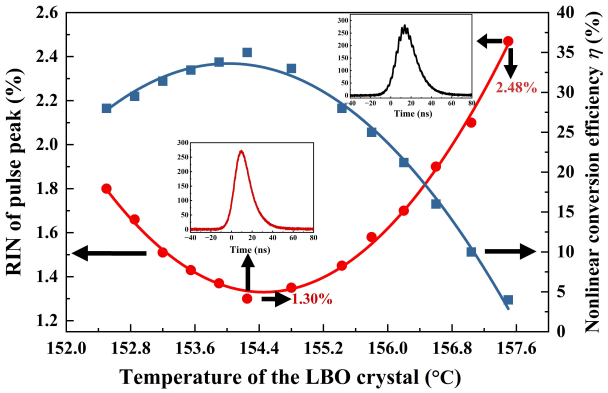

Fig. 8. The measured values of RIN and η as a function of the temperature of the LBO crystal.

When the nonlinear conversion efficiency is maximum, the pulse train becomes more stable compared to the pulse train without nonlinear loss, as shown in Fig. 9(a). Statistical histograms of pulse amplitude voltage showed a narrow, high Gaussian distribution for the stabilized pulse train, with the distribution width reduced from 80 mV to 20 mV, as shown in Fig. 9(b).

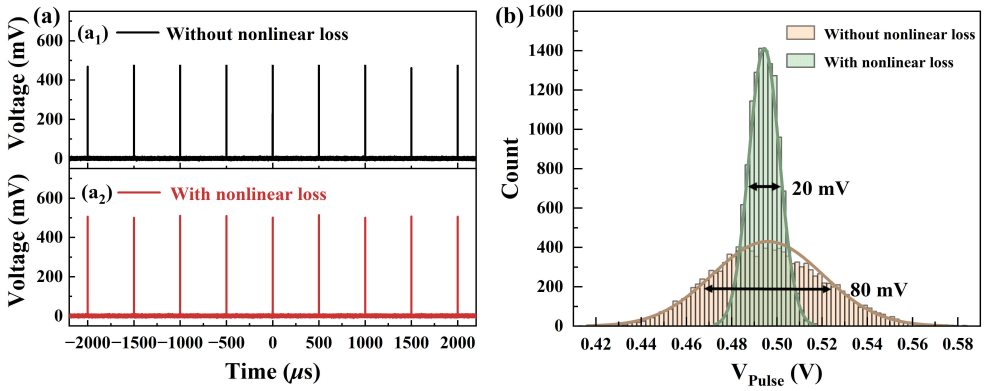

Fig. 9. Comparison of pulse trains (a) and amplitude statistical histograms with and without NOFC (b).

The long-term stability of pulse peak and pulse energy were recorded over a total duration of 2.25 hours, where 165,000 pulse sequence samples were collected. The calculated RIN for the 1064 nm pulsed laser was 1.30% (Fig. 10(a)). One noise source that must be considered in the measurement is quantization error, which arised from the digitization of the input signal in the measurement equipment. The experiment used an oscilloscope with a 12-bit analog-to-digital converter (ADC), providing 4096 discrete voltage levels and introducing a maximum error of 1/4096, corresponding to a noise contribution of approximately 0.03%. After subtracting this quantization error, the corrected RIN value for the 1064 nm pulsed laser was 1.27%. The pulse energy stability over the 2.25 hours period was 0.09%, as shown in Fig. 10(b).

Optics EXPRESS

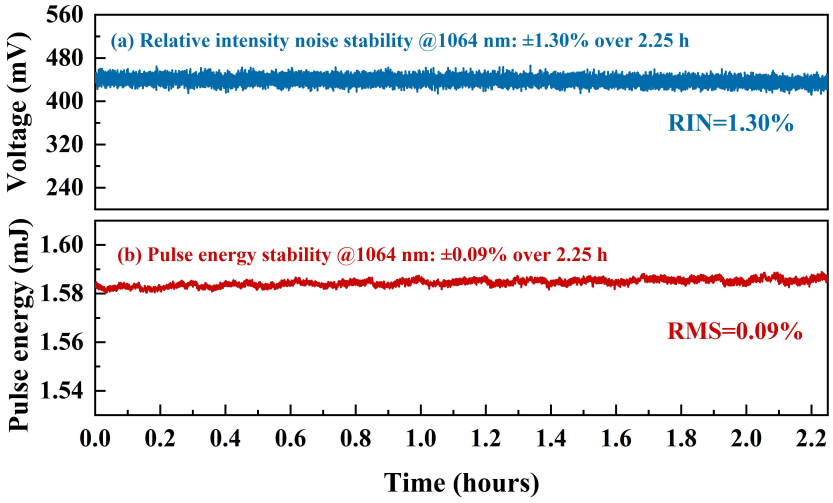

Fig. 10. Stability characterization of 1064 nm pulsed laser. (a) relative intensity noise; (b) pulse energy.

Based on the noise suppression methods described above, a low RIN 1064 nm pulsed laser was realized with a repetition rate of 1 kHz, an average output power of 1.58 W, as shown in Fig. 11(a). The pulse width of the 1064 nm laser, as measured by a high-speed photoelectric detector was 18.85 ns, as shown in Fig. 11(b), corresponding to a peak power of 84.65 kW and a pulse energy of 1.58 mJ. The beam quality factors were measured using a beam profiler, yielding $M_x^2 = 1.02$ and $M_y^2 = 1.05$, as shown in Fig. 11(c).

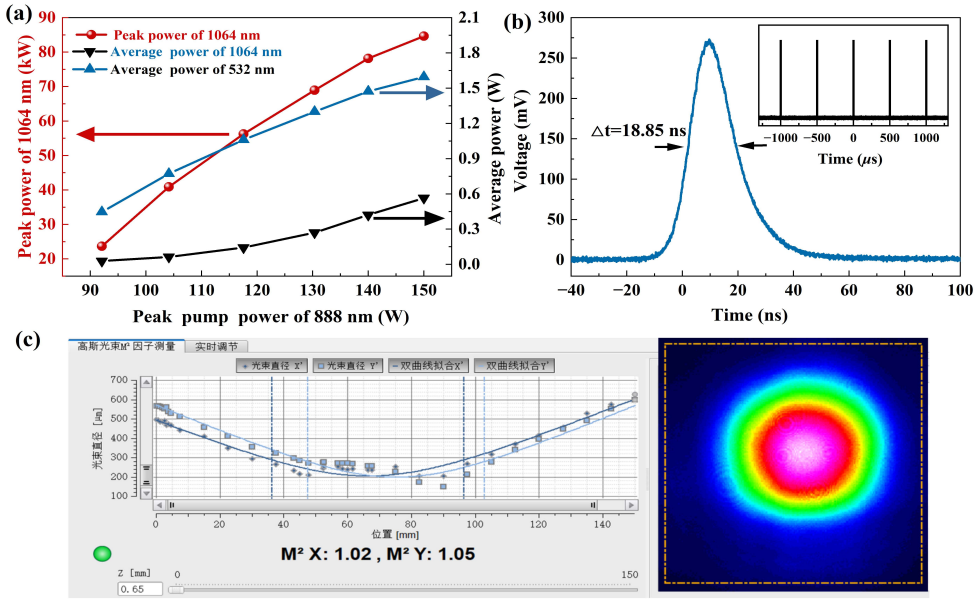

Fig. 11. Characterization of a 1064 nm pulsed laser. (a) output power; (b) pulse width and pulse train; (c) beam quality.

Optics EXPRESS

5. Conclusions

This paper presented a method for reducing the RIN of actively Q-switched pulsed laser, which was implemented by combining the RO and NOFC to effectively suppress pulse-to-pulse RIN. The diffraction loss of AO Q-switch was slightly lowered to introduce the RO process. As a result, the inverted population at the beginning of pulse building-up was stabilized to a constant value by the RO process, thereby ensuring initial gain consistently per pulse. The RIN was reduced from 4.90% to 2.48% by optimizing the diffraction loss and the RO duration. On this basis, to further suppress the intensity fluctuation arising from DLM beating with random phases, a noncritical phase-matched nonlinear crystal LBO was introduced into the cavity to introduce nonlinear loss. By optimizing the LBO crystal temperature to improve the nonlinear conversion efficiency, the RIN was further decreased to 1.27% (after ADC quantization error correction). Ultimately, a low intensity noise 1064 nm laser was realized with a repetition rate of 1 kHz, a pulse energy of 1.58 mJ and a pulse width of 18.85 ns, corresponding to a peak power of 84.65 kW. The beam quality M^2 in x and y directions were 1.02 and 1.05, respectively. Compared to other methods of reducing pulse-to-pulse RIN, such as seed laser injection, it didn't require additional seed laser, thus reducing the complexity of the laser system. In addition, it reduced the RIN by directly resetting the initial laser dynamics rather than relieving the fluctuation of the already generated pulse sequence, thus eliminating noise fluctuations source more effectively. The low noise pulsed laser presented here is suitable for many important fields including high-speed fiber-optic communications, precision Light Detection and Ranging (LiDAR) systems, and various optical sensing technologies where signal integrity is paramount.

Funding. National Natural Science Foundation of China (62575163); National Key Research and Development Program of China (2022YFC2204003); The First Lab - National Innovation Center (Shanxi) science and technology innovation project; Funding from the National Key Laboratory of Particle Transport and Separation Technology (KWKF-2024-2).

Disclosures. The authors declare no conflict of interest.

Data availability. Data underlying the results presented in this paper are not publicly available at this time but may be obtained from the authors upon reasonable request.

References

1. D. J. Wineland and W. M. Itano, "Laser cooling of atoms," Phys. Rev. A **20**(4), 1521–1540 (1979).
2. Y.-F. Huang, B.-H. Liu, L. Peng, *et al.*, "Experimental generation of an eight-photon Greenberger–Horne–Zeilinger state," Nat. Commun. **2**(1), 546 (2011).
3. W. Peng, P. Jin, F. Li, *et al.*, "A review of the high-power all-solid-state single-frequency continuous-wave laser," Micromachines **12**(11), 1426 (2021).
4. Y. Wei, W. Peng, J. Li, *et al.*, "Self-mode-matching compact low-noise all-solid-state continuous wave single-frequency laser with output power of 140 W," Opt. Lett. **48**(3), 676–679 (2023).
5. S. Greenstein and M. Rosenbluh, "The influence of nonlinear spectral bandwidth on single longitudinal mode intra-cavity second harmonic generation," Opt. Commun. **248**(1-3), 241–248 (2005).
6. H. Lu, J. Su, Y. Zheng, *et al.*, "Physical conditions of single-longitudinal-mode operation for high-power all-solid-state lasers," Opt. Lett. **39**(5), 1117–1120 (2014).
7. H. Lu, X. Sun, M. Wang, *et al.*, "Single frequency Ti:sapphire laser with continuous frequency-tuning and low intensity noise by means of the additional intracavity nonlinear loss," Opt. Express **22**(20), 24551–24558 (2014).
8. H. Lu, Y. Guo, and K. Peng, "Intensity noise manipulation of a single-frequency laser with high output power by intracavity nonlinear loss," Opt. Lett. **40**(22), 5196–5199 (2015).
9. A. E. Amili and M. Alouini, "Noise reduction in solid-state lasers using a SHG-based buffer reservoir," Opt. Lett. **40**(7), 1149–1152 (2015).
10. F. Saltarelli, A. Diebold, I. J. Graumann, *et al.*, "Self-phase modulation cancellation in a high-power ultrafast thin-disk laser oscillator," Optica **5**(12), 1603–1606 (2018).
11. N. Bode, F. Meylahn, and B. Willke, "Sequential high power laser amplifiers for gravitational wave detection," Opt. Express **28**(20), 29469–29478 (2020).
12. X. Zhang, J. Ye, X. Luo, *et al.*, "148-W single-frequency Nd:YAG Innoslab μs-amplifier at 1064 nm with high efficiency," Opt. Express **29**(4), 5687–5693 (2021).
13. S. Schiemann, A. Kuhn, S. Steuerwald, *et al.*, "Efficient coherent population transfer in NO molecules using pulsed lasers," Phys. Rev. Lett. **71**(22), 3637–3640 (1993).

Optics EXPRESS

14. P. Benedetti, G. Cristoforetti, S. Legnaioli, *et al.*, "Effect of laser pulse energies in laser induced breakdown spectroscopy in double-pulse configuration," Spectrochim. Acta, Part B **60**(11), 1392–1401 (2005).
15. Y.-L. Chen, J. Lewis, and C. Parigger, "Spatial and temporal profiles of pulsed laser-induced air plasma emissions," J. Quant. Spectrosc. Radiat. Transfer **67**(2), 91–103 (2000).
16. X. Wang, C. Ma, C. Li, *et al.*, "Influence of pulse energy on machining characteristics in laser induced plasma micro-machining," J. Mater. Process. Technol. **262**, 85–94 (2018).
17. J. A. Morris and C. R. Pollock, "Passive Q switching of a diode-pumped Nd:YAG laser with a saturable absorber," Opt. Lett. **15**(8), 440–442 (1990).
18. S. Matsuo, L. Yan, J. Si, *et al.*, "Reduction of pulse-to-pulse fluctuation in laser pulse energy using the optical Kerr effect," Opt. Lett. **37**(10), 1646–1648 (2012).
19. H. Zhang, D. Li, P. Shi, *et al.*, "Efficient, high power, Q-switched Nd:YLF slab laser end-pumped by diode stack," Opt. Commun. **250**(1-3), 157–162 (2005).
20. Y. Zhang, P. Jin, J. Yang, *et al.*, "Spectral purity improvement of high-power pulsed lasers achieved by manipulating the nonlinear optical frequency conversion," Opt. Lett. **50**(10), 3341–3344 (2025).